Ceramics International (xxxx) xxxx–xxxx

Contents lists available at ScienceDirect

Ceramics International

journal homepage: www.elsevier.com/locate/ceramint

# $Li_2ZnTi_3O_8$ based High κ LTCC tapes for improved thermal management in hybrid circuit applications

S. Arun[a], M.T. Sebastian[b], K.P. Surendran[a,*]

[a] Materials Science and Technology Division, National Institute for Interdisciplinary Science and Technology, CSIR, Trivandrum 695019, India
[b] Microelectronics Research Unit, Faculty of Information Technology and Electrical Engineering, University of Oulu, 90014 Finland

ARTICLE INFO

*Keywords:*
LTCC
Tape casting
Thermal conductivity
Dielectric materials/properties
Thermal expansion

ABSTRACT

A low temperature co-fired ceramic based on $Li_2ZnTi_3O_8$ (LZT), that possess auspicious thermal and dielectric properties is reported. In order to achieve the low sintering temperature suitable for LTCC applications (875 °C), 1 wt% of 20:$Li_2O$-20: MgO-20: ZnO-20:$B_2O_3$-20: $SiO_2$ (LMZBS) glass was added to LZT ceramics. The post-milled powder had an average particle size of 450 nm with an effective surface area of 0.812 $m^2g^{-1}$. A well dispersed tape casting slurry was prepared using xylene/ethanol mixture as solvent and fish oil as dispersant. The crystal structure and microstructure of the tapes were analyzed through XRD and scanning electron microscopy (SEM). The microwave dielectric properties of the green as well as sintered tapes were measured at different frequencies (5, 10 and 15 GHz). The $Li_2ZnTi_3O_8$+1 wt% LMZBS has shown excellent thermal conductivity of 5.8 W/mK, thermal expansivity (11.97 ppm/°C) closer to silver electrode, low temperature coefficient of dielectric constant (−29 ppm/°C) and ultralow dielectric losses (tanδ~$10^{-4}$).

## 1. Introduction

The size reduction trend of hand held electronic devices have now grown into newer dimensions with the advent of hybrid circuit concept, which is realized by embedding passive components at the intermediate layers, giving ample room to mount active components on the surface of the multilayer structure. In this direction, low temperature co-fired ceramic (LTCC) technology has attracted much attention because of its ease of design and functional benefits due to excellent electrical performance, partly contributed by enabling highly conductive electrode metals like Ag, Cu, Au etc [1–3]. For an ideal material to be qualified for LTCC applications, besides lower sintering temperature ( < 950 °C), it should possess low dielectric constant ($\varepsilon_r < 10$), low dielectric loss (tanδ < $10^{-3}$), tolerable coefficient of thermal expansivity (CTE) with respect to electrodes ( < 20 ppm/°C) and high thermal conductivity ( > 10 W/mK). Surprisingly enough, most of the commercial LTCC substrate possesses CTE close to silicon ( < 5 ppm/°C), which can exert thermal stress on passive components due to the former's higher thermal expansivities ( > 15 ppm/°C). Secondly, achieving high thermal conductivity is also harder to realize, since most of the ceramics have lower thermal conductivities, which gets further lowered with the addition of glasses. Nonetheless, any material that qualifies to show a thermal conductivity above 5 W/mK is really appreciable since they can partly eliminate thermal vias in certain specific LTCC applications.

Lowering the sintering temperature without deteriorating the dielectric properties is the principal hurdle towards the goal of developing a successful LTCC material. In general, plenty of techniques are available to lower the sintering temperature of ceramic materials such as addition of glasses and low melting oxides as sintering aids, chemical processing, using smaller particles as the starting materials and so for [4]. Recent works suggest that, the use of a proper low loss and low temperature melting glass as a sintering aid, is the most suitable approach in this direction [5,6]. It was reported that multicomponent glasses are more effective than single component glasses in the aspect of possessing better dielectric properties. The selection of a suitable sintering aids is of prime importance, because in some cases the addition of an improper glass may deteriorate the microwave dielectric properties besides aggravating the grain growth, which permits some ions from glassy phase to substitute at the matrix lattice and form satellite phases [7].

Commercial LTCC materials in general, are found to possess low dielectric constants ($\varepsilon_r < 10$), which pose little freedom to microelectronic circuit designers. However, certain specific applications such as microwave filters demand high dielectric constant LTCC tapes as substrates in hybrid circuits. It should be noted that non ferroelectric, high dielectric constant, but low loss LTCC substrates are advantageous since they have smaller levels of cross talk. Interestingly, there is a

* Corresponding author.
*E-mail address:* kpsurendran@niist.res.in (K.P. Surendran).

http://dx.doi.org/10.1016/j.ceramint.2017.01.073
Received 21 November 2016; Received in revised form 6 January 2017; Accepted 14 January 2017

surprising scarcity of literature on high dielectric constant LTCC materials except a few studies like Zhou et al. who developed a $Bi_2Mo_2O_9$ based LTCC material with high dielectric constant [8]. Recently a few high dielectric constant compositions of ultra-low temperature co-fired ceramics (ULTCC) based on $(1-x)BiVO_4$-$xTiO_2$ (x=0.4, 0.50, 0.55 and 0.60) were also reported [9]. Other than these isolated research and development reports, LTCC tapes with high dielectric constant ($\varepsilon_r > 20$) are not at all available in the commercial market. The present paper is a candid attempt in this direction to develop a novel LTCC substrate possessing $\varepsilon_r > 21$ in the sintered form, along with a combination of low dielectric loss and interesting thermal and mechanical characteristics. This kind of LTCC materials can also serve as a buffer layer between piezoelectric laminates (a passive component) and low loss dielectric laminates (a signal processing component), in periodic multilayer structures.

Recently, a resurged interest was generated on the spinel structured $Li_2ZnTi_3O_8$ based ceramic system because of their comparatively low sintering temperature (1075 °C) and excellent dielectric properties [10–12]. Blasse *et al.* in 1963 reported $Li_2ZnTi_3O_8$ for the first time. Later, its stoichiometry and crystal structure have been investigated by Hernandez *et al.* [9,12] In 2010 Sumesh *et al.* reported the microwave dielectric properties of $Li_2ZnTi_3O_8$ sintered at 1075 °C for the first time ($\varepsilon_r$=25.6, $Q_u$xf=72000 GHz and $\tau_f$=−11.2 ppm/°C) [12]. Huang *et al.* investigated the effect of Mg and Co doping on the microwave dielectric properties of $Li_2ZnTi_3O_8$. They obtained high Q factor for the compositions $Li_2(Zn_{0.94}Mg_{0.06})Ti_3O_8$ ($Q_u$xf=150000 GHz) and $Li_2(Zn_{0.92}Co_{0.08})Ti_3O_8$ ($Q_u$xf=140000 GHz) [13]. Subsequently, a lot of research work was carried out on different LTCC compositions involving $Li_2ZnTi_3O_8$ [14,15]. Recently, Sumesh and Sebastian reported the microwave dielectric properties of $Li_2ZnTi_3O_8$+1 wt% LMZBS glass composite [16]. The bulk ceramic composite sintered at 925 °C has a dielectric constant of 24.3, $Q_u$xf=58000 GHz with a $\tau_f$ of −11 ppm/°C. Besides, the said composite is chemically compatible with silver electrode material. In the present study, we have employed a non aqueous based tape casting technique, in order to develop $Li_2ZnTi_3O_8$+1 wt% LMZBS (LZT+LMZBS) glass composite as a candidate material for high κ LTCC applications. The structural, microstructural, thermal, dielectric and mechanical properties of the newly developed LTCC tape sintered at 875 °C were analyzed. In comparison with the commercial LTCC products, the new LTCC material has a higher coefficient of linear expansivity (CTE) and thermal conductivity, that can complement to enhance their reliability.

## 2. Experimental

### 2.1. Preparation of LZT+LMZBS glass composite

$Li_2ZnTi_3O_8$ (LZT) was synthesized by solid state ceramic route using high purity $Li_2CO_3$ (99%), ZnO (99.9%), and $TiO_2$ (99.8%) from Aldrich (St. Louis. MO, USA) as the starting materials. Stoichiometric amounts of all these chemicals were ball milled together in ethanol medium using yttria stabilized zirconia balls for 24 h. The slurry was then dried overnight in a hot air oven at a temperature of 100 °C and was calcined at a temperature of 900 °C in a high temperature furnace with a dwell time of 4 h. In order to bring down the sintering temperature of LZT, 1 wt% LMZBS glass (20:$Li_2O$ 20: MgO 20: ZnO, 20:$B_2O_3$, 20: $SiO_2$) was added to it. Prior to this, LMZBS glass powder was prepared from high-purity chemicals of $B_2O_3$ (99%, Sigma-Aldrich), $Li_2CO_3$, $SiO_2$ (99.6%, Sigma-Aldrich), ZnO and $(MgCO_3)_4.Mg(OH)_2{\cdot}5H_2O$ (99.9% Sigma-Aldrich) using the splash quenching method and then made into fine powder. The ceramic powder was then added together with 1 wt% LMZBS and ball milled in ethanol medium for 24 h for homogenous mixing of the ceramic and glass powders, for further reduction in the particle size. The phase purity of the as prepared LZT+LMZBS was studied by powder X- ray diffraction using Ni filtered Cu *Kα* radiation (PANalytical X′pert PRO diffractometer, Almelo, Netherlands). The average particle size was characterized by dynamic light scattering (Zetasizer Nanoseries: ZEN 3600, Malvern, Worcestershire, UK) and the BET surface area of LZT +LMZBS powder was estimated using surface area analyzer (Gemini 2375, Micromeritics, Norcross, USA). The CTE of the LZT+LMZBS were analyzed using a thermo mechanical analyzer (TMA SS7300, SII Nano Technology Inc, Northridge, CA, USA) respectively. The linear thermal expansion coefficient ($\alpha_l$) was calculated in the temperature range of $T_1 < T < T_2$, by the following equation.

$$\alpha_l = \frac{L_2 - L_1}{L_1(T_2 - T_1)} \tag{1}$$

where $L_1$ and $L_2$ are the lengths of the specimen at temperature$T_1$ and$T_2$ respectively. The thermal conductivity of the sintered ceramic of LZT+LMZBS was directly measured by a xenon flash technique using laser flash thermal properties analyzer (FlashLine2000, Anter Corporation, Pittsburgh, USA) where the relevant portion of a suitably shaped ceramic specimen (thickness=2.72 mm and diameter=12.67 mm) is heated locally using an IR flash gun. The specific heat of the sample can be calculated by assuming that the energy absorbed by the sample and a standard reference sample are the same and is given by,

$$C_{sample} = \frac{(mC\Delta T)_{ref}}{(m\Delta T)_{sample}} \tag{2}$$

Thermal diffusivity ($D$) is calculated by the instrument by measuring $t_{50}$ (half rise time), time for the back face temperature to reach 50% of its maximum value and the relationship between $D$ and $t_{50}$ is given by the famous Parker relation as [17],

$$D = \frac{0.139a^2}{t_{50}} \tag{3}$$

where a is the thickness of the sample. From the measured value of $D$, C and known value of density (ρ), the thermal conductivity $K$ can be calculated by the below equation,

$$K = DC\rho \tag{4}$$

### 2.2. Preparation of LZT+LMZBS tape

For a uniform and homogenous tape preparation, the viscosity of the slurry should be optimized to yield maximum colloidal stability. Initially, sedimentation stability studies were conducted by keeping the powder loading constant at 50 wt% and varied the amount of dispersant. Here, fish oil (Arjuna Natural Extracts, Kerala, India) was used as the dispersant. The slurry preparation was done in two stages; in the first stage, the powder is mixed with dispersant and xylene/ethanol (50:50) solvent system and was ball milled for one day. In the second stage it was added with polymeric binder (poly vinyl butyral, (PVB) (Sigma–Aldrich)) and two types of plasticizers, benzyl butyl phthalate (Sigma–Aldrich) and poly ethylene glycol (Sigma–Aldrich), were added to provide strength and flexibility to the green tape. A few drops of cyclohexanone (Sigma–Aldrich) was used as the homogenizer. The dispersant was optimized by measuring the viscosity of the slurry in the first stage by varying the concentration of fish oil from 0.5 to 2 wt%. The viscosity measurements were carried out by using a rheometer (Brookfield, R/S Plus, MA, USA). The slurry with an optimal balance of the filler, solvents, dispersants and plasticizers was casted into thin ceramic tapes of approximate thickness 50 μm using a tape casting machine (Keko equipment, Zuzemberk, Slovenia) on a silicon coated Mylar® film, employing double doctor blade technique [18]. The thermal decomposition profile of the green tape was examined using thermo gravimetric analyzer, TG (Perkin Elmer, Waltham, USA). The dried green tapes were cut and thermolaminated (14 layers) at a temperature of 70 °C under a pressure of 5 MPa for 15 min. The hot

pressed thick samples were sintered at a temperature of 875 °C for 2 h. The microhardness of the sintered tape of LZT+LMZBS was measured by Vicker's microindentation hardness test (Shimadzu HMV-2TAW, Kyoto, Japan). Vicker's hardness test or diamond-pyramid hardness test of the LZT+LMZBS is usually conducted with a square base diamond pyramid as the indenter and the angle between the opposite phases of the indenter is typically 136° [19]. The Vickers hardness number (*VHN*) or diamond pyramid hardness number (DPH) is obtained by dividing the applied load by the surface area of the indentation and is given by the relation as follows [20,21].

$$VHN = \frac{2PSin(\frac{\theta}{2})}{L^2} \quad (5)$$

where $P$ is the applied load, $L$ is the average length of the diagonal (mm) obtained from the indentation and $\theta$ is the angle between the opposite faces of the indenter. Using optical microscopy the length of the diagonal ($L$) can be measured. From the known values of $P$ and $\theta$, average value of VHN can be calculated. The microstructure of the green, sintered and co-fired samples were analyzed using scanning electron microscopy, SEM (JOEL-JSM 5600 LV, Tokyo, Japan). The surface roughness of the green and sintered samples was measured using atomic force microscopy, AFM (Bruker, Nano, USA) in the tapping mode. The low frequency dielectric properties of bulk LZT +LMZBS (Diameter=11.97 mm and Thickness=1.92 mm) were measured using Hioki 3532-50 LCR Hi tester, Japan. The microwave dielectric properties of the sintered tape were measured in a split post dielectric resonator (QWED, Warsaw, Poland) operating at frequencies 5, 10 and 15 GHz with the aid of a Vector Network Analyzer (E5071C, Agilent Technologies, Santa Clara, CA). The temperature coefficient of dielectric constant ($\tau_\varepsilon$) of the sintered LZT+LMZBS tape was measured using SPDR with an arrangement for heating the entire set up in the temperature range of 25–60 °C. The variation in the resonant frequency and quality factor was noted for every 3 °C rise in temperature and $\tau_\varepsilon$ was determined using the formula [22],

$$\tau_\varepsilon = \frac{\Delta\varepsilon}{\varepsilon\Delta T} \quad (6)$$

where $\varepsilon$ is the initial dielectric constant and $\Delta\varepsilon$ is the change in dielectric constant during the change in temperature $\Delta T$.

## 3. Results and discussion

### 3.1. Properties of LZT+LMZBS glass ceramic

Lithium zinc titanate belongs to the spinal family having $AB_2O_4$ structure, where A and B refers to the cations in the tetrahedral and octahedral positions respectively. Two different structure configurations are possible for a spinal, namely $A(B_2)O_4$ distribution and the inverse spinel, $B(AB)O_4$, where the parenthesis represents octahedral site position. The system $Li_2O–ZnO–TiO_2$, crystallizes in cubic spinel crystal structure with space group $P4_332$. Fig. 1(a) shows the XRD pattern of LZT+LMZBS glass tape sintered at 875 °C. It is clear that the addition of LMZBS and subsequent heat treatment did not lead to the formation of secondary phases. All the peaks in XRD can be indexed based on JCPDS file number 86–1512 with cubic crystal symmetry. The particle size and surface area are two important parameters of the ceramic powder for fabricating a uniform and homogenous green tape. The average particle size obtained for the final LZT+LMZBS powder is 450 nm (Fig. 1(b)) and the BET surface area is 0.812 $m^2/g$, which are within agreeable limits suitable for slurry preparation.

Fig. 2(a) shows the thermal expansion characteristics of LZT +LMZBS from room temperature to 400 °C. In a typical ceramic material, the coefficient of linear thermal expansion is very low due to the strong interatomic bonding as compared to polymers and metals [23,24]. In printed circuit board technology (PCB) the high resistance

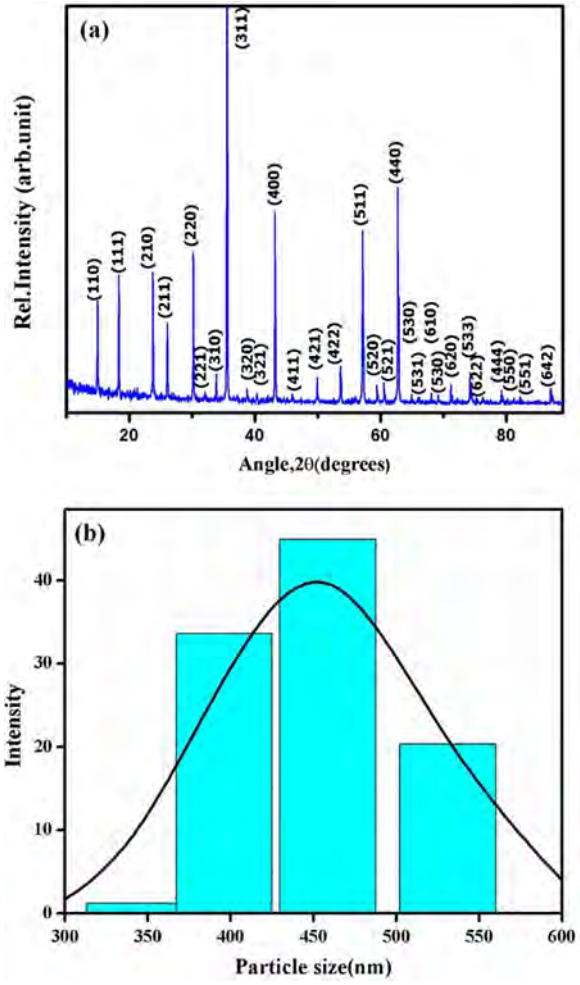


**Fig. 1.** (a) XRD pattern of LZT+LMZBS tape sintered at 875 °C and (b) particle size distribution of LZT+LMZBS glass.

loss offered by complex wire circuitry is a major drawback. This can be reduced in LTCC technology by integrating high conductivity metallic interconnects within the substrate itself. In hybrid circuits managing thermal delamination is a major challenge. In order to circumvent the risk of delamination while co-firing, it is better to use a ceramic having matching CTE with that of the metals. It should be noted that most of the LTCC materials are designed to set their CTE values close to that of silicon i.e. between 2–5 ppm/°C, in order to accommodate the surface mounted silicon chips. But in hybrid circuits, most of the metals like Au, and Ag have high CTE ( > 10 ppm/°C). On scanning through the literature, one could see only very few reports on LTCC materials possessing a CTE > 10 ppm/°C. For example, Chen et al. reported a higher CTE value of 11.7 ppm/°C for an LTCC system based on quartz+ $BaO-Al_2O_3-SiO_2-B_2O_3$ composite [25]. In comparison with other LTCC materials, the new LZT+LMZBS composite possess an unusually higher CTE value of 11.97 ppm/°C.

In a typical hybrid device like pressure sensor mounted on steel surface, the thermal expansivity of the functional LTCC module should match with that of the metal, to get the desired reliability [26]. Furthermore, due to the recent progress in passive integration, we may need new LTCC materials with high permittivity and CTE for burying a variety of inductors and capacitors. Against this background, the development of a high CTE LTCC substrate can be beneficial. As discussed elaborately in literature, heat is inevitably developed in all hybrid electronic circuits which have to be removed from the devices for their safety. Although LTCC technology possesses thermal conductivity ranges 10 times larger than organic laminates, it is still one

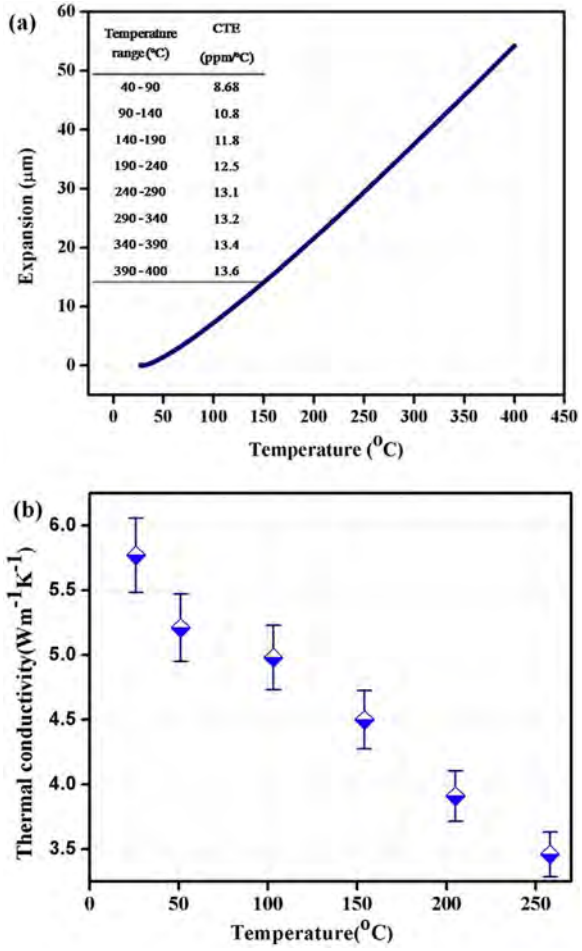


**Fig. 2.** (a) Thermal expansion characteristics and (b) Thermal conductivity measurements of LZT+LMZBS bulk sintered at 900 °C.

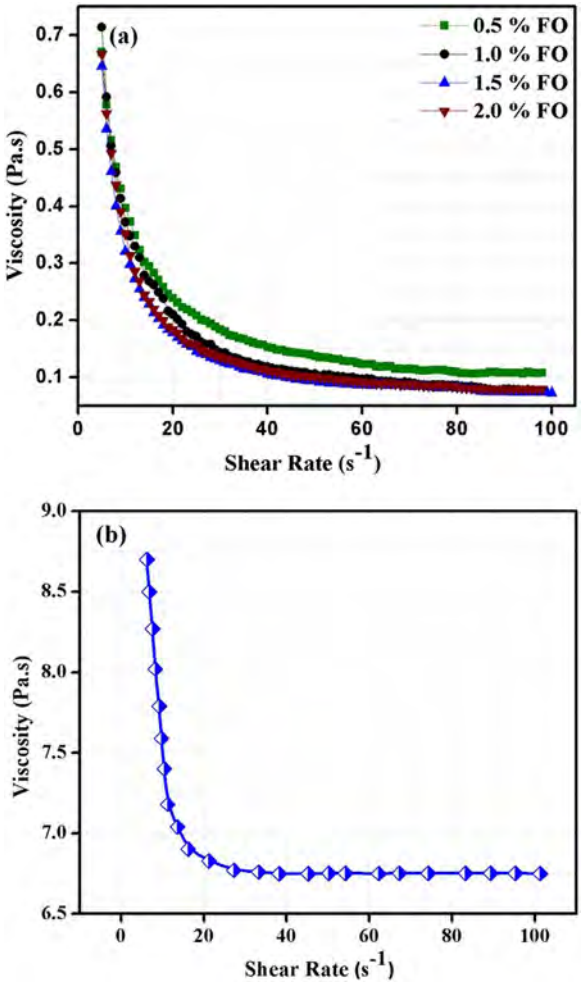


**Fig. 3.** (a) Variation of viscosity with different fish oil (FO) concentration with respect to weight of the powder (b) Variation of viscosity of the ready-to-cast LZT+LMZBS tape casting slurry, as a function of shear rate.

order less than alumina based HTCC substrates. The present hybrid circuit uses thermal vias for heat management that inevitably make the circuit design more complicated. Hence it is clear that LTCC technology is badly looking for high thermal conductivity substrates [27]. From Fig. 2(b), it is clear that thermal conductivity has a maximum value of 5.8 W/mK which decreases as temperature increases from room temperature. This trend is obvious for all ceramic materials above Debye temperature, that the thermal conductivity is inversely proportional to the temperature. Recently Induja *et al.* obtained a thermal conductivity value of 7.2 W/mK which is for an alumina based system [28]. In comparison to commercial alumina based tapes, the present LZT+LMZBS substrate is advantageous, since it possess a relatively high thermal conductivity of 5.8 W/mK at room temperature, which can partly eliminate thermal vias for specific applications.

### 3.2. Characteristics of LZT+LMZBS tapes

The control of flow characteristics of the slip is crucial in every tape casting process, wherein the slurry selected for tape casting should be well dispersed and homogenous. Non aqueous tape casting protocols are widely used because the employment of low volatile organic solvents enable fast drying. Beside, this method can avoid hydration of the ceramic particles [29,30]. The first step in a typical slip preparation involves selection of a suitable solvent system that should follow certain conditions like proper evaporation rate, low cost, and it should be capable to dissolve all the organic additives like binder, plasticizer, homogenizer etc. in the slurry [31].

In this work, a xylene/ethanol binary solvent system was used to dissolve the organic moieties in the slurry. The selected solvent system has a high evaporation rate compared to other organic solvents. Fish oil is used as the dispersant to disperse particles through steric stabilization. The main reason for using PVB as binder in the present research is due to its outstanding green tape characteristics, as reported in several studies before [31]. Over and above, the binder should provide pseudoplastic behavior to the slurry [30,32]. In order to impart flexibility to the green tape, plasticizers were added to the slurry. Glycols and phthalates are commonly used as plasticizers, that are compatible with poly vinyl butyral binder [31]. The selection of the two types of plasticizers is also critical since they should soften the monomeric bonds of the polymeric binder. In the current report, benzyl butyl phthalate and poly ethylene glycol were chosen as the type I and type II plasticizers. It is understood that ceramic slurries especially with heavy solid loading should have a shear dependent viscosity, which is suitable to analyze its flow behavior by considering it as a non Newtonian fluid.

Fig. 3(a) shows the variation of the viscosity of the slurry as a function of shear rate. It is believed that the fish oil (FO) disperses the ceramic particle through steric stabilization that prevents them from settling [33]. From above figure, it is evident that the viscosity decreases with increase in shear rate and a minimum value is obtained for 1.5 wt% of fish oil. The observation of higher viscosity for the lower value of dispersant is believed to be due to the insufficient amount of dispersant to disperse the particles. As shown, beyond 1.5 wt% of the fish oil, the viscosity rises again which is believed to be contributed by

**Table 1**
Final composition of the tape casting slurry.

| Component | Composition (wt%) | Function |
|---|---|---|
| **First stage** | | |
| LZT+LMZBS | 47.1 | Filler |
| Fish oil | 0.71 | Dispersant |
| Xylene | 23.6 | Solvent |
| Ethanol | 23.6 | Solvent |
| **Second stage** | | |
| Poly vinyl butyral | 2.3 | Binder |
| Benzyl butyl phthalate | 1.2 | Plasticizer (Type I) |
| Polyethylene glycol | 1.2 | Plasticizer (Type II) |
| Cyclohexanone | 0.3 | Homogenizer |

the bridging flocculation [34]. In to this optimum composition, pre-calculated amounts of binder, plasticizers and homogenizers were added to transform the slurry suitable for tape casting (see Table 1). Fig. 3(b) depicts the flow characteristic of the ready-to be-casted slurry. This slurry with balanced composition clearly follows a pseudo plastic behavior, which can also be due to the presence of layer of liquid vehicle in between the ceramic particle that reduces the viscosity [35]. In other words, shear thinning occurs due to the breaking up of these solid-solid bonds with the increase in shear rate [34]. It should be remembered that this trend in the viscosity is a primary prerequisite for effective tape casting since after passing beyond the blade there is no shear force [36]. Hence the slurry viscosity will increase after passing the blade and the mobility of the constituent particle decreases [37]. Table 1 shows the composition of the final tape casting slurry of LZT+LMZBS.

The thermal decomposition of the organic matter and the resultant shrinkage is to be controlled strictly, which otherwise would result in cracks, warpage etc. We employed thermogravimetric (TG) analysis as an effective tool to estimate the different organic removal stages of a casted green tape. Ideally, the organic additives should be removed completely before the sintering, otherwise it will adversely affect the shrinkage and the material properties of the sintered ceramic [38,39]. The TG measurement was conducted from room temperature to 700 °C at a heating rate of 10 °C/min. As the temperature increased from room temperature, initially there observed a slow weight loss of 1% up to 200 °C. The main contribution for the gravimetric weight loss in this temperature range is due to the burnout of low molecular weight organic additives like dispersant and plasticizers. From 200–425 °C, there is a sudden weight loss of 9%, mainly due to the exhaustion of organic binders present in it [30,40,41]. Based on the systematic analysis of the decomposition of the slurry components revealed through TG analysis, a sintering profile suitable for the LZT+LMZBS tape is designed as shown in Fig. 4(b). The sintered tape is observed to have a shrinkage of 7%, 8% and 12% in the x, y and z axes respectively. To reduce the warping of the sintered substrates, constrained sintering techniques were employed by keeping a suitable designed porous alumina plate on top of the green substrate during the firing stage.

Determination of the mechanical properties like Vicker's hardness and Young's modulus of an LTCC ceramic are of particular interest, since glass contents in them diminish their hardness which delimit the machinability of substrates for electronic components [42]. This is because LTCC operations like punching vias, wire bonding etc. may impart mechanical stresses on these substrates, which should have the strength to stand these stresses. In a typical microindentation testing, the microscopic analysis of the indentation area before and after the indentation will be analyzed that can give vital information on the deformation and fracture mechanism [43]. The optical microscopic image of the surface of the indented LZT+LMZBS substrate sintered at 875 °C for 2 h is shown in Fig. 5(a). The average value VHN after five measurements is obtained as 278.21 with a standard deviation of 23.47. In standard units, the hardness of LZT+LMZBS glass tapes

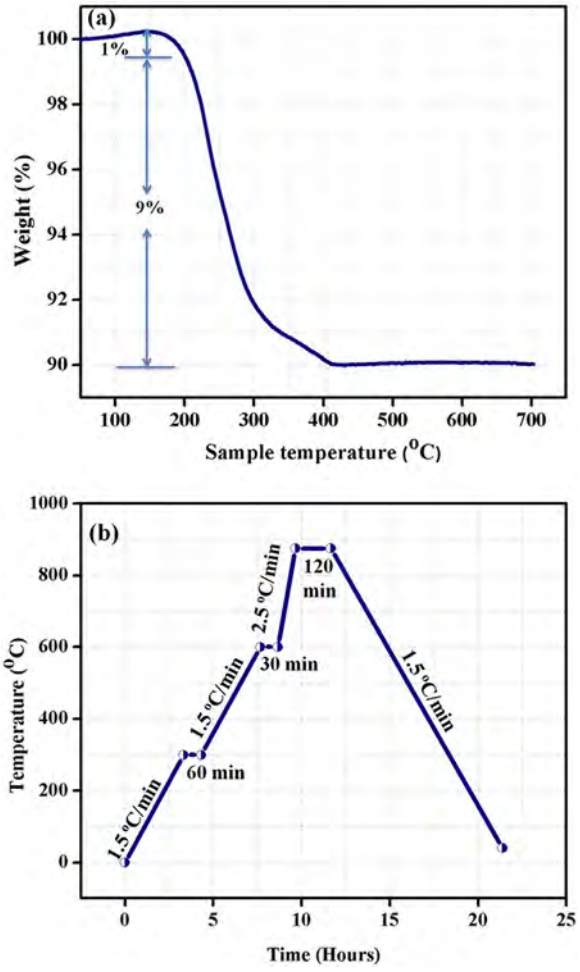


**Fig. 4.** (a) Thermogravimetric analysis of LZT+LMZBS green tape in the range 25–700 °C and (b) sintering profile for LZT+LMZBS green tape.

varies between 2.498–2.959 GPa. Tandonet al. measured the micro-hardness of sintered tapes of Dupont 951 using a Vicker's indentation technique and achieved a value of 7.36 GPa [44].

SEM images of the surfaces and cross section of the green and sintered tapes of LZT+LMZBS are shown in Fig. 6. Fig. 6(a) shows the surface of the green tape, where one can notice that the ceramic particles are bonded together by the polymeric binder with an average particle size of the ceramic approximated to be 1 μm. The cross section of the sintered tape is displayed in the Fig. 6(b). Finally in 6(c) the microstructure of the sintered surface is depicted, which on closer inspection illustrates the presence of glassy phase in melted form. The average grain size ranges from less than 3–4 μm with a more or less uniform distribution. Fig. 6(d) represents scanning electron micro-graph of the surface of screen printed Ag paste on the surface of LZT +LMZBS green tape. Plate like microstructure is observed throughout the surface with most of the Ag particles possessing triangle like morphology. As shown, presence of scattered black portions found in Fig. 6(d) indicates the porous nature in the printed pattern. Diffusion of the Ag into the substrate material and its partial evaporation from the material surface are the two key challenges that will encounter while co-firing ceramic with Ag in LTCC technology. In order to test the diffusion of Ag into the LTCC tape matrix, Ag paste was blanket printed on top of two green tapes and subsequently thermolaminated them altogether. Ag paste after sintering at 875 °C for 2 h transforms from trigonal shape to a well densified polyhedral microstructure. The microstructure cross section of the co-fired LZT+LMZBS tapes (see Fig. 6(f)) also testifies that there were no visible diffusion of Ag towards the interior of material even after sintering. The presence of void spaces

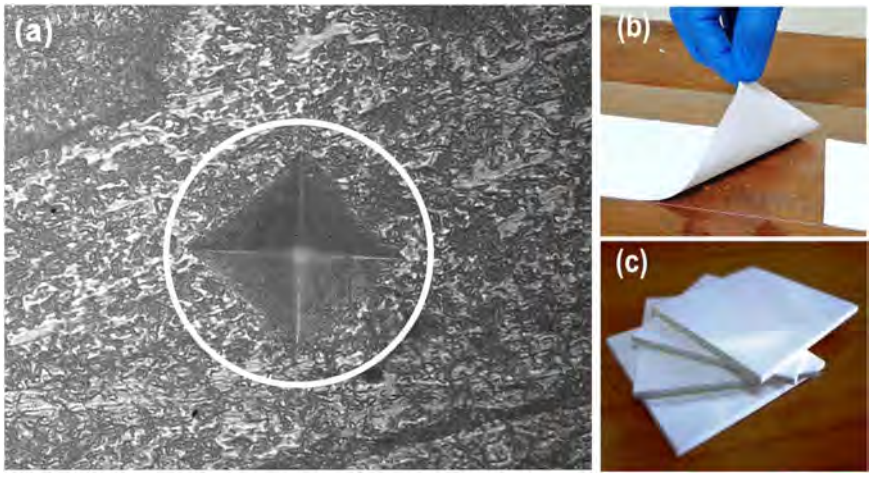


**Fig. 5.** (a) Optical microscopic image of the indentation produced by Vicker's indenter on the surface of LZT+LMZBS tape sintered at 875 °C (b) Photograph of the surface of the green tape of LZT+LMZBS (single layer) peel off from the carrier film (c) photograph of substrates of LZT+LMZBS sintered by stacking 25 green single layers.

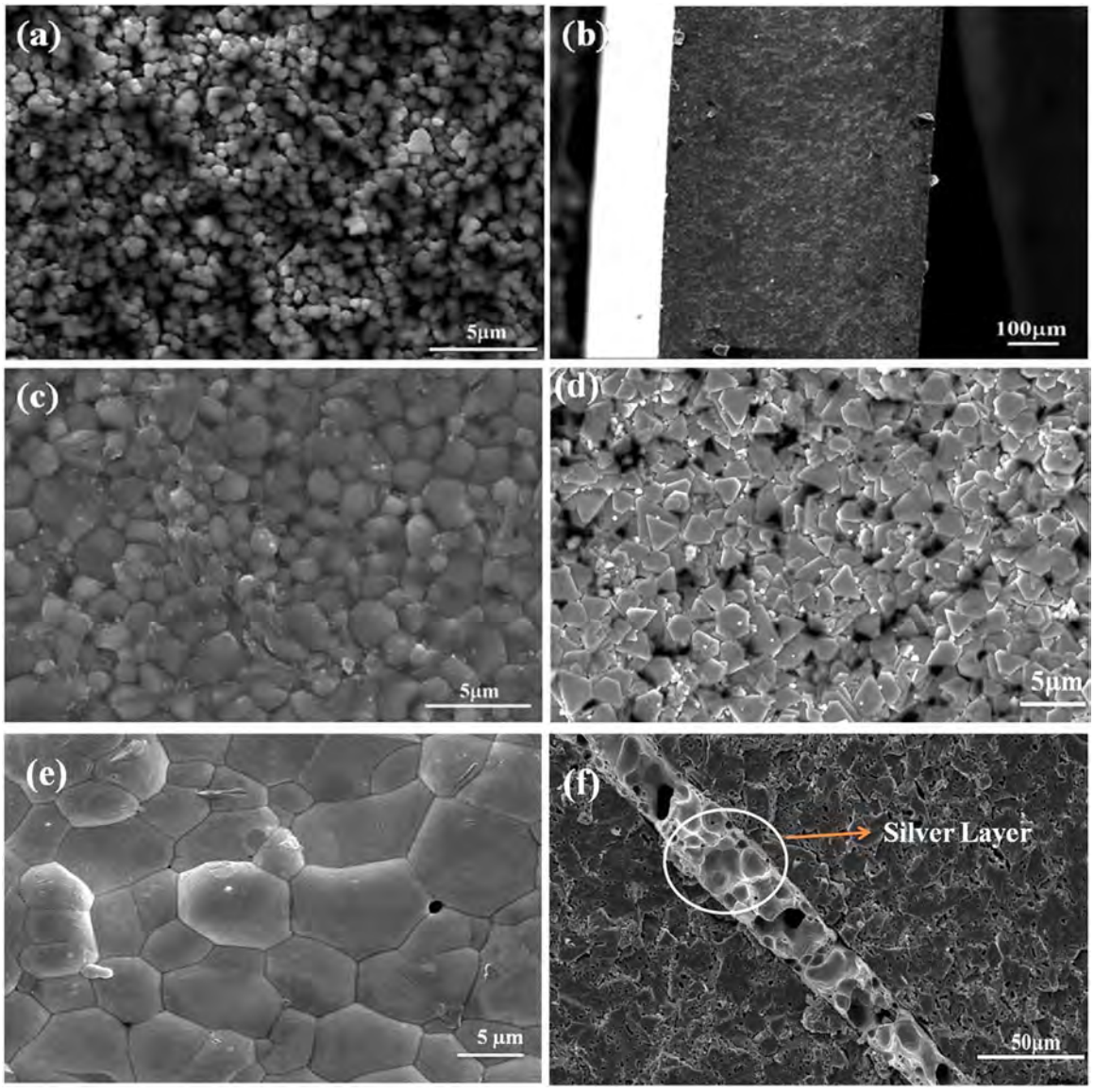


**Fig. 6.** SEM images of the (a) surface of the green tape, (b) cross section of the tape sintered at 875 °C and (c) its surface, (d) surface of the screen printed Ag paste on LZT+LMZBS green tape, prior to co-firing, (e) surface of the Ag screen printed tape after co-firing (875 °C) and (f) cross section of the stacked tape with embedded Ag paste, after thermolamination and co-firing.

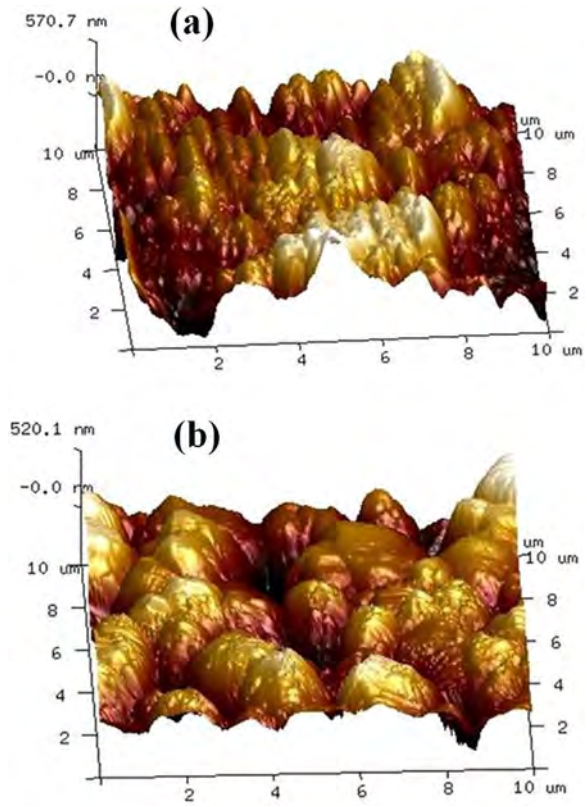


**Fig. 7.** AFM images of (a) surface of green tape and (b) surface of sintered tape (875 °C) of LZT+LMZBS.

in the co-fired silver layer in Fig. 6(f) is attributed to the burning out of some organic additives from the silver paint. Hence it can be summarized that Ag based passive components can be co-fired with LZT+LMZBS LTCC substrate in hybrid electronic circuits.

Fig. 7 shows the AFM images of the surfaces of green and sintered tapes of LZT+LMZBS. The green body has an average surface roughness of 151 nm while that of the sintered one is around 128 nm. The skewness and curtosis values of the green and sintered tapes were estimated as −0.107 & 2.96 for green and −1.14 & 4.13 for sintered tape respectively. The negative value of skewness indicates that valleys are predominant on the surface of the sintered tape. In the present study, the kurtosis value obtained indicate that the surface has finite roughness within the permissible limits which is essential for effective adhesion of the metallic conductor during metallization [45].

Fig. 8(a) shows the variation of the dielectric constant of the sintered LTCC tape as a function of ambient to 60 °C measured at 5 GHz using SPDR. The calculated value of temperature coefficient of dielectric constant ($\tau_\varepsilon$) is −29 ppm/°C. The comparatively lower value of $\tau_\varepsilon$ of LZT+LMZBS tape, is a clear indicative of the temperature stability of the newly developed LTCC substrate, when it is used in multilayer microwave modules. Finally, the LZT+LMZBS tape is characterized for dielectric properties both at RF and microwave frequency ranges. The low frequency (100 Hz–5 MHz) response of the LZT+LMZBS bulk is shown in Fig. 8(b). LZT+LMZBS has a dielectric constant of 24.14 and dielectric loss of $5.1\times10^{-4}$ at 1 MHz.

Table 2 summarizes the microwave dielectric properties of the thermolaminated LZT+LMZBS green and sintered tapes at frequencies 5, 10 and 15 GHz. Obviously the green tape has a lower value of relative permittivity compared to its sintered ones, which is mainly due to the presence of pores and organic additives like binders, plasticizers and homogenizers. Most of the organic moieties have high dielectric loss but low dielectric constant, due to their strong covalent bonding and lower atomic polarizabilities. During sintering, the porosity is decreased significantly consequent to the burnout of organics and the

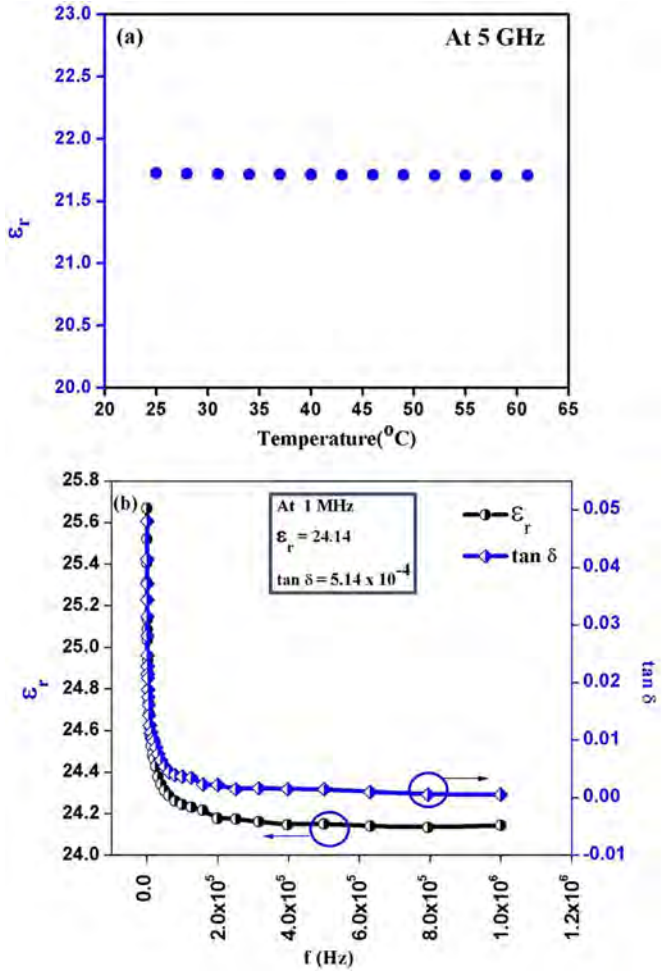


**Fig. 8.** (a) Variation of dielectric constant with temperature and (b) low frequency dispersion of $\varepsilon_r$ and tanδ of LZT+LMZBS bulk sintered at 900 °C.

material undergo densification to a coherent rigid ceramic. This will in turn improve the relative permittivity and reduces the dielectric loss compared to the green ones. It should be noted that at 5 GHz, the sintered LZT+LMZBS tape of 546 nm thickness shows a dielectric constant, $\varepsilon_r$=21.9 and dielectric loss, tanδ=$6\times10^{-4}$. This kind of high $\varepsilon_r$ LTCC substrates are useful in microwave filters and also as a buffer layer for piezoelectric LTCC laminate in a periodic multilayer structure.

## 4. Conclusion

LZT+LMZBS prepared by solid state ceramic route was used as the filler for the preparation of LTCC tape casting slurry. Rheological studies reveal that in the first stage of the slurry preparation 1.5 wt% fish oil is optimum amount as a dispersant, with respect to the ceramic powder. This will get modified to 0.71 wt% with respect to the total weight of the slurry, when suitable amounts of plasticizers, binder and homogenizer were added in the second stage. Uniform and homogeneous slurry was tape casted on to Mylar® substrate, using double doctor blade technique. The apparent CTE value of 11.97 ppm/°C ideally suits the new LTCC substrate to be co-fired with high conductivity metals like Ag, Cu and Au, without visible delamination. The thermal conductivity value of 5.8 W/mK was observed for the LZT +LMZBS ceramic, which has been the highest, in comparison to commercial LTCC substrates. The relatively higher thermal conductivity and thermal expansivity helps the tape to achieve better thermal management in hybrid circuits like LTCC filters. The surface morphology of the as prepared thermolaminated sintered tape was studied

**Table 2**
Microwave dielectric properties of LZT+LMZBS Green and Sintered Tape.

| Material | No. of layers | Thickness (μm) | Dielectric properties at | | | | | |
|---|---|---|---|---|---|---|---|---|
| | | | 5 GHz | | 10 GHz | | 15 GHz | |
| | | | $\varepsilon_r$ | tanδ | $\varepsilon_r$ | tanδ | $\varepsilon_r$ | tanδ |
| Laminated stack | 14 | 623 | 9.5 | 0.0556 | 9.4 | 0.0500 | 9.2 | 0.0603 |
| Sintered stack | 14 | 546 | 21.9 | 0.0002 | 21.5 | 0.0004 | 21.3 | 0.0007 |

using SEM and AFM techniques. The dielectric properties of the sintered tape of LZT+LMZBS was found to be $\varepsilon_r$=21.9, $\tau_\varepsilon$ =−29 ppm/°C and tanδ=6×10$^{-4}$ at 5 GHz. Such LTCC tapes with high thermal conductivity, high CTE, moderately high dielectric constant and low dielectric loss are also suitable as a buffer layer in hybrid transducer applications.

## Acknowledgements

Authors are grateful for the financial support from the DST funded project (File no: DST/TSG/NTS/2012/89). The authors are also thankful to Dr. P. Prabhakar Rao and Mr. M. R. Chandran for extending SEM and XRD, Dr. Yoosaf Karuvath and Mr. Aswin for the AFM, and Mr. A. Peer Mohamed for TG and BET facilities.

## References

[1] J.J. Bian, J.Y. Wu, Designing of glass-free LTCC microwave ceramic- $Ca_{1-x}(Li_{0.5}Nd_{0.5})_xWO_4$ by crystal chemistry, J. Am. Ceram. Soc. 95 (2012) 318–323.
[2] J. Guo, C.A. Randall, G. Zhang, D. Zhou, Y. Chen, H. Wang, Synthesis, structure, and characterization of new low-firing microwave dielectric ceramics: $(ca_{1-3x}Bi_{2x}\Phi_x)MoO_4$, J. Mater. Chem. C. 2 (2014) 7364–7372.
[3] M.T. Sebastian, H. Jantunen, Low loss dielectric materials for LTCC applications: a review, Int. Mater. Rev. 53 (2008) 57–90.
[4] L. Fang, C. Su, H. Zhou, Z. Wei, H. Zhang, Novel low-firing microwave dielectric ceramic $LiCa_3MgV_3O_{12}$ with low dielectric loss, J. Am. Ceram. Soc. 96 (2013) 688–690.
[5] T. Joseph, M.T. Sebastian, H. Jantunen, M. Jacob, H. Sreemoolanadhan, Tape casting and dielectric properties of $Sr_2ZnSi_2O_7$-based ceramic-glass composite for low-temperature co-fired ceramics applications, Int. J. Appl. Ceram. Technol. 8 (2011) 854–864.
[6] P.S. Anjana, M.T. Sebastian, Microwave dielectric properties and low-temperature sintering of cerium oxide for LTCC applications, J. Am. Ceram. Soc. 92 (2009) 96–104.
[7] H. Naghib-Zadeh, C. Glitzky, W. Oesterle, T. Rabe, Low temperature sintering of barium titanate based ceramics with high dielectric constant for LTCC applications, J. Eur. Ceram. Soc. 31 (2011) 589–596.
[8] D. Zhou, C.A. Randall, A. Baker, H. Wang, L.X. Pang, X. Yao, Dielectric properties of an ultra-low-temperature cofiring $Bi_2Mo_2O_9$ multilayer, J. Am. Ceram. Soc. 1446 (2010) 1443–1446.
[9] D. Zhou, D. Guo, W.B. Li, L.X. Pang, X. Yao, D.W. Wang, I.M. Reaney, Novel temperature stable high-$\varepsilon_r$ microwave dielectrics in The $Bi_2O_3$ –$TiO_2$ –$V_2O_5$ system, J. Mater. Chem. C. 4 (2016) 5357–5362.
[10] G. Blasse, The structure of some new mixed metal oxides containing lithium, J. Inorg. Nucl. Chem. 743 (1963) 1473–1474.
[11] V.S. Hernandez, L.M.T. Martinez, G.C. Mather, A.R. West, Stoichiometry, Structures and Polymorphism of spinel like phases, $Li_{1.33x}Zn_{2-2x}Ti_{1+0.67x}O_4$, J. Mater. Chem. 6 (1996) 1533–1536.
[12] S. George, M.T. Sebastian, Synthesis and microwave dielectric properties of novel temperature stable high Q, $Li_2ATi_3O_8$ (A=Mg, Zn) ceramics, J. Am. Ceram. Soc. 93 (2010) 2164–2166.
[13] C. Huang, C. Su, C. Chang, High Q microwave dielectric ceramics in the $Li_2(Zn_{1-x}A_x)Ti_3O_8$(A=Mg, Co; X=0.02-0.1) system, J. Am. Ceram. Soc. 94 (2011) 4146–4149.
[14] Y. Li, Z. Qin, B. Tang, S. Zhang, G. Chang, H. Li, H. Chen, H. Yang, J. Li, Microwave dielectric properties of $TiO_2$ added $Li_2ZnTi_3O_8$ ceramics doped with $Li_2O$-$Al_2O_3$-$B_2O_3$ glass, J. Electron. Matter 44 (2015) 281–286.
[15] X. Lu, Y. Zheng, B. Zhou, Z. Dong, P. Cheng, Microwave dielectric properties of $Li_2ZnTi_3O_8$ ceramics doped with $Bi_2O_3$, Ceram. Int. 39 (2013) 9829–9833.
[16] S. George, M.T. Sebastian, Low-temperature sintering and microwave dielectric properties of $Li_2ATi_3O_8$ (A=Mg, Zn) ceramics, Int. J. Appl. Ceram. Technol. 8 (2011) 1400–1407.
[17] W.J. Parker, R.J. Jenkins, C.P. Butler, G.L. Abbott, Flash method of determining thermal diffusivity, heat capacity, and thermal conductivity, J. Appl. Phys. 32 (1961) 1679–1684.
[18] R.E. Mistler, E.R. Twiname, Tape Casting: theory and Practice, American Ceramic Society, Wiley, Westerville, Ohio, 2000.
[19] C.B. Ponton, R.D. Rawlings, Vickers indentation fracture toughness test. Part 1. Review of literature and formulation of standardised indentation toughness equations, Mater. Sci. Technol. 5 (1989) 865–872.
[20] R. Tickoo, R.P. Tandon, K.K. Bamzai, P.N. Kotru, Microindentation studies on samarium-modified lead titanate ceramics, Mater. Chem. Phys. 80 (2003) 446–451.
[21] A. Sakar-Deliormanli, M. Güden, Microhardness and fracture toughness of dental materials by indentation method, J. Biomed. Mater. Res. B. Appl. Biomater. 76 (2006) 257–264.
[22] O. Dernovsek, A. Naeini, G. Preu, W. Wersing, M. Eberstein, W.A. Schiller, LTCC glass-ceramic composites for microwave application, J. Eur. Ceram. Soc. 21 (2001) 1693–1697.
[23] W.D. Kingery, Introduction to Ceramics, John Wiley & Sons,Inc, Ny, USA, 1960.
[24] W.D. Callister, D.G. Rethwisch, Fundamentals of Materials Science and Engineering an Introduction, 8th ed, John Wiley & Sons, Inc, US, 2001.
[25] S. Chen, S. Zhang, X. Zhou, B. Li, Thermal and dielectric properties of The LTCC composites based on The eutectic system BaO–$Al_2O_3$–$SiO_2$–$B_2O_3$, J. Mater. Sci. Mater. Electron. 22 (2011) 238–243.
[26] M. Eberstein, C. Glitzky, M. Gemeinert, T. Rabe, W.A. Schiller, C. Modes, Design of LTCC with high thermal expansion, Int. J. Appl. Ceram. Technol. 6 (2009) 1–8.
[27] T. Thelemann, H. Thust, G. Bischoff, T. Kirchner, Liquid cooled LTCC substrates for high power applications, Int. J. Microcircuits Electron. Packag. 23 (2000) 209–214.
[28] I.J. Induja, P. Abhilash, S. Arun, K.P. Surendran, M.T. Sebastian, LTCC tapes based on $Al_2O_3$–BBSZ glass with improved thermal conductivity, Ceram. Int. 41 (2015) 13572–13581.
[29] D. Hotza, P. Greil, Review: aqueous tape casting of ceramic powders, Mater. Sci. Eng. A. 202 (1995) 206–217.
[30] D. Thomas, P. Abhilash, M.T. Sebastian, Casting and characterization of $LiMgPO_4$ glass free LTCC tape for microwave applications, J. Eur. Ceram. Soc. 33 (2013) 87–93.
[31] P. Boch, T. Chartier, Understanding and improvement of ceramic processes: the example of tape casting, Mater. Sci. Forum 34–36 (1991) 813–819.
[32] C.A. Gutiérrez, R. Moreno, Tape casting of non-aqueous silicon nitride slips, J. Eur. Ceram. Soc. 20 (2000) 1527–1537.
[33] A.C. Ali, E. Suvaci, H. Mandal, Role of organic additives on non-aqueous tape tasting of SiAlON ceramics, J. Eur. Ceram. Soc. 31 (2011) 167–173.
[34] L. Palmqvist, O. Lyckfeldt, E. Carlström, P. Davoust, A. Kauppi, K. Holmberg, Dispersion mechanisms in aqueous alumina suspensions at high solids loadings, Colloid Surf. A 274 (2006) 100–109.
[35] S. Li, Q. Zhang, H. Yang, D. Zou, Fabrication and characterization of $Li_{1+x-y}Nb_{1-x-3y}Ti_{x+4y}O_3$ substrates using aqueous tape casting process, Ceram. Int 35 (2009) 421–426.
[36] T.C. Paton, Paint Flow and Pigment Dispersion: A Rheological Approach to Coating and Ink Technology, 2nd ed, John Wiley & Sons, US, 1964.
[37] L.A. Salam, R.D. Matthews, H. Robertson, Optimisation of thermoelectric green tape characteristics made by the tape casting method, Mater. Chem. Phys. 62 (2000) 263–272.
[38] M.J. Cima, J.A. Lewis, A.D. Devoe, Binder distribution in ceramic greenware during thermolysis, J. Am. Ceram. Soc. 72 (1989) 1192–1199.
[39] L.A. Salam, R.D. Matthews, H. Robertson, Pyrolysis of Polyvinyl Butyral (PVB) Binder in Thermoelectric Green Tapes, J. Eur. Ceram. Soc. 20 (2000) 1375–1383.
[40] S. Lüftl, B. Balluch, W. Smetana, S. Seidler, Kinetic study of the polymeric binder burnout in green Low temperature co-fired ceramic tapes, J. Therm. Anal. Calorim. 103 (2011) 157–162.
[41] P.M. Geffroy, T. Chartier, J.F. Silvain, Innovative approach to metal matrix composites film by tape casting process, Adv. Eng. Mater. 9 (2007) 547–553.
[42] O.I. Pushkarev, Study of The surface strength and crack resistance of very hard ceramic materials by The microindentation method, Refract. Ind. Ceram. 43 (2002) 295–298.
[43] B.R. Lawn, D.B. Marshal, Hardness, toughness, and brittleness: anan indentation analysis, J. Am. Ceram. Soc. 62 (1979) 347–350.
[44] R. Tandon, C.S. Newton, S.L. Monroe, S.J. Glass, C.J. Roth, Sub-critical crack growth behavior of a low temperature co-fired ceramic, J. Am. Ceram. Soc. 90 (2007) 1527–1533.
[45] P. Abhilash, M.T. Sebastian, K.P. Surendran, Glass free, non-aqueous LTCC tapes of $Bi_4(SiO_4)_3$ with high solid loading, J. Eur. Ceram. Soc. 35 (2015) 2313–2320.